AJNR

Pseudohemangioma of the Vertebra: An Unusual Radiographic Manifestation of Primary Ewing's Sarcoma

Joshua A. Bemporad, Gordon Sze, John C. Chaloupka and Charles Duncan

This information is current as of August 7, 2025.

AJNR Am J Neuroradiol 1999, 20 (10) 1809-1813
http://www.ajnr.org/content/20/10/1809

AJNR Am J Neuroradiol 20:1809–1813, November/December 1999

Case Report

Pseudohemangioma of the Vertebra: An Unusual Radiographic Manifestation of Primary Ewing's Sarcoma

Joshua A. Bemporad, Gordon Sze, John C. Chaloupka, and Charles Duncan

Summary: Primary Ewing's sarcoma (ES) of the spine is uncommon, exhibiting a variety of appearances on plain-film radiographs and cross-sectional images. We report the unusual CT imaging manifestations of a primary ES with a coarse trabecular pattern that mimicked an aggressive hemiangioma of the cervical spine.

Ewing's sarcoma (ES) is an aggressive malignant neoplasm accounting for 6% to 8% of all primary bone tumors (1). Involvement of the spinal column is typically seen in advanced stages of the disease, usually representing widespread metastases (2). In contrast, primary ES of the nonsacral spine is uncommon, representing approximately 0.9% of cases (3). Primary involvement of the spine may produce a variety of imaging manifestations that can mimic other diseases, often resulting in delays in appropriate treatment. We report the unusual imaging findings of a primary ES of the cervical spine that mimicked an aggressive vertebral hemangioma.

Case Report

An 8-year-old boy presented with 1 month of progressive neck pain associated with weakness and paresthesias of both arms. The pain was initially localized to the neck and upper back, worsened with extension, and was partly relieved by heat and acetaminophen. Two weeks before admission, he developed diffuse right-sided wrist pain with rare episodes of left-sided wrist pain.

On examination he had a low-grade temperature (37.4° C) and held his neck in a flexed position. There was point tenderness of the lower cervical spine with limited range of motion. There was bilateral upper extremity weakness and intact sensation. Initial laboratory values were normal (complete blood cell count with differential, sedimentation rate, prothrombin time, and partial thromboplastin time).

Plain films showed expansion of the left C6–7 neural foramen with smooth, sclerotic margins and a partial compression fracture of C7 (Fig 1). Noncontrast CT showed a coarse trabecular pattern of the body of C7 (Fig 2). A dumbbell-shaped epidural soft-tissue mass was seen extending out of the left neural foramen. There was associated moderate spinal cord compression posteriorly. A CT scan of the chest was normal, without any evidence of pulmonary nodules or lymphadenopathy.

To evaluate these findings better, an MR image of the cervical spine was obtained. This confirmed the C7 compression and epidural mass noted on prior imaging. The lesion exhibited low signal on T1-weighted images and intermediate-to-high signal on T2-weighted images (Figs 3 and 4). The lesion enhanced heterogeneously (Fig 5), and displaced both the dural sac and left vertebral artery (Fig 6). The remainder of the spine and brain appeared normal.

Given the absence of lymphadenopathy or metastatic lesions, a working diagnosis at that time was an aggressive hemangioma producing a compression fracture and epidural mass at C7. This led to a referral for a spinal angiogram to confirm the diagnosis and for possible preoperative embolization. Spinal arteriography showed mild but abnormal hypervascularity within the corpus of C7, with paraspinal staining of the left neural foramen at the level of the previously revealed epidural tumor (Fig 7). There was no arteriovenous shunting to suggest a malignant process. As the angiographic findings were nonspecific and not particularly characteristic for vertebra hemangioma, no preoperative embolization was performed.

A radionuclide bone scan was done to look for other areas of involvement. Whole-body planar images after injection of technetium-99m methylene diphosphonate showed only a slight focal area of increased activity at the level of C7. It was uncertain whether this was related to the lesion or to the compressive deformity, as seen by CT.

With a primary diagnosis of a vascular tumor, the patient underwent operative resection and stabilization consisting of C6–7 and C7–T1 diskectomies, C7 corpectomy, epidural tumor resection, C6–T1 fusion with anterior C6–T1 plating, and halo placement. Histologic examination of the mass (Fig 8) showed small, round-to-oval, hyperchromatic cells with pyknotic nuclei and scanty cytoplasm. There were areas of necrosis with scattered mitotic figures. Immunohistochemical analysis was positive for CD99 and negative for LCA and PGP 9.5. These findings were characteristic of the diagnosis of Ewing's sarcoma.

The patient was started on cytoxan, doxorubicin, vincristine, and G-CSF. Sixteen days after the operation, the patient was discharged home in good condition. At the time of writing this, 20 months later, the patient has had no evidence of recurrence.

Discussion

Primary ES of the spine is rare. In a frequently cited study, Whitehause and Griffiths reviewed 1020 cases of ES and found an incidence of 3.5% for the whole spine and 0.9% for the nonsacral spine (3). The average age of primary spinal ES has been reported to be 16.5 years; however, 88% of patients are 20 years or younger (1). ES is the second most common primary bone malignancy in children after osteosarcoma (4). There is a male predominance and 90% of patients are younger

Received November 19, 1998; accepted after revision July 7, 1999.

From the Departments of Diagnostic Radiology (J.A.B., J.C.C., G.S.) and Neurosurgery (J.C.C., C.D.), Yale University School of Medicine, New Haven, Connecticut.

Address reprint requests to Gordon Sze, MD, Department of Diagnostic Radiology, Yale-New Haven Hospital, 333 Cedar Street, New Haven, CT 06504.

© American Society of Neuroradiology

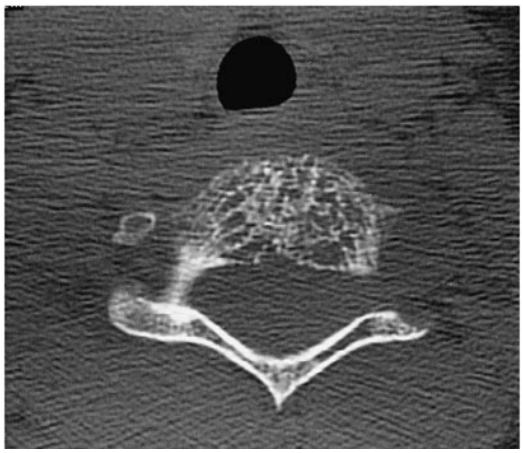

FIG 1. Lateral plain film of lower cervical spine shows compression of C7 vertebra with preservation of C6–7 disk space.

FIG 2. Axial CT scan without contrast (*bone window*) shows course trabecular pattern with disruption of cortex of vertebral body. Left neural foramen is slightly widened.

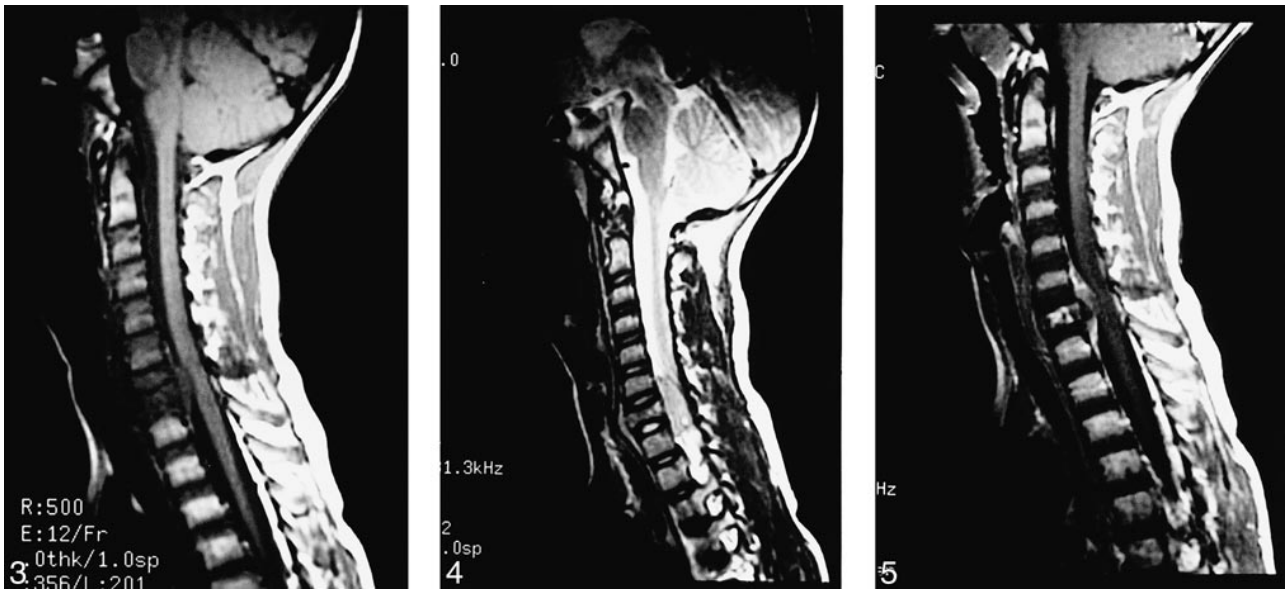

FIG 3. Midline sagittal T1-weighted image of cervical spine shows homogeneous extradural mass compressing spinal cord posteriorly. Mass is low in signal and roughly isointense to gray matter. C7 vertebra is compressed and is decreased in signal with preservation of intervertebral disk spaces.

FIG 4. Sagittal T2-weighted image of cervical spine slightly to left of midline better shows preservation of intervertebral disk spaces. Extradural mass is fairly homogeneous and intermediate-to-high in signal. Compression of C7 vertebra with increase in anteroposterior diameter is obvious.

FIG 5. Midline sagittal T1-weighted image with contrast shows heterogeneous enhancement of extradural mass and C7 vertebral body. There is no abnormal enhancement of the spinal cord.

than 30 years of age. It is rare in black persons (5). Ewing's sarcoma usually involves the bones of the lower extremity and pelvis but virtually any bone in the body can be affected. It commonly metastasizes to lungs, other bones, and lymph nodes (6).

Primary ES of the spine can present with a clinical triad of back pain, neurologic defect, and palpable mass (7). In a study of 22 patients, 14 had a neurologic deficit related to spinal cord or nerve root compression, four had a palpable mass, and all but one presented with back pain (8). In that study,

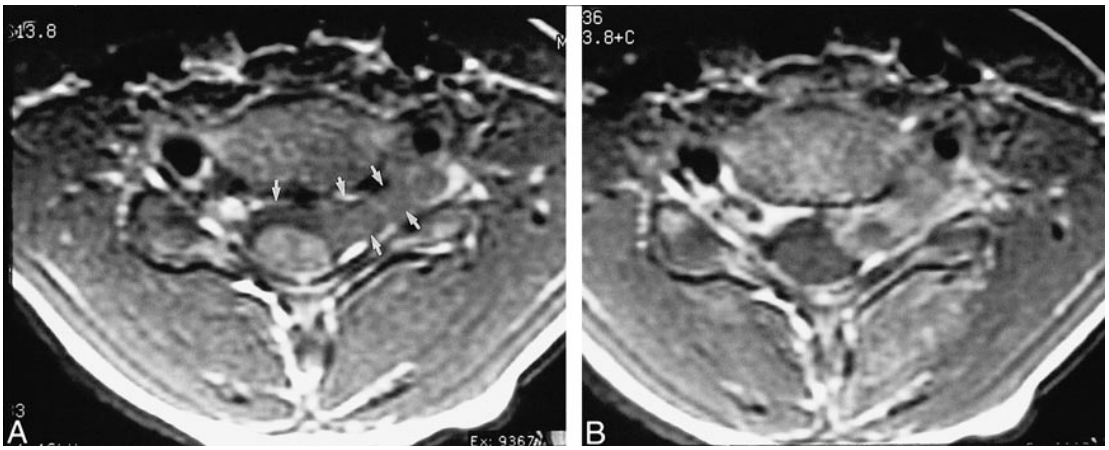

FIG 6. *A,* T1-weighted axial image through C6–7 intervertebral disk shows extradural mass compressing spinal cord posteriorly. Mass crosses midline and extends out of left neural foramen (*arrows*).
B, T1-weighted axial image with contrast shows heterogeneous enhancement of mass.

FIG 7. Superselective angiogram of left costocervical trunk. Late arterial-phase projection shows staining in region of epidural mass.

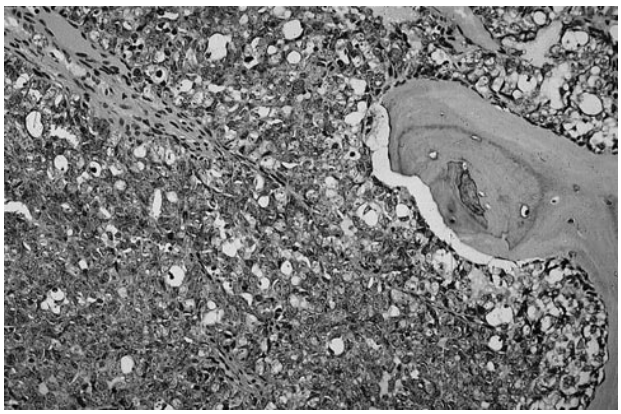

FIG 8. Photomicrograph reveals that tumor is composed of densely packed small, round-to-oval cells (*lower left*) with high nuclear-to-cytoplasmic ratio (''small blue cell tumor;'' several representative cells are highlighted with small *arrowheads*). Tumor has infiltrated medullary space of vertebrae. Note bone spicule (*letter A*) on right of figure. Faint thin-walled vascular channels are present (outlined by *large arrowheads*) (hematoxylin and eosin, original magnification × 200). Cells were immunopositve for CD99 and immunonegative for LCA and PGP 9.5. (not shown).

the mean duration of symptoms was 2½ months (8). Those with lesions involving the rostral spine often present earlier than those in the caudal spine or sacrococcygeal area (2, 8). Constitutional signs and symptoms such as fever, anemia, weight loss, and leukocytosis often occur.

The origin of ES remains uncertain, although current research suggests that it is probably an undifferentiated neoplasm of neuroectodermal origin (5). ES cells grown in culture show no evidence of differentiation. On gross pathologic inspection, ES tumors are soft, pink-to-gray tumors with foci of hemorrhage and necrosis. An extraosseous portion of the neoplasm is present in more than 80% of cases and is usually much larger then the intraosseous component (6). Areas of hemorrhage and necrosis are common.

Radiographic and CT appearances of primary ES of the spine are variable. Lesions may be lytic, sclerotic, or mixed with associated partial or complete vertebral compression (1). Usually the radiographic appearance is that of osteolysis with partial collapse. Osteosclerosis is uncommon. When it occurs, it is usually patchy, but dense osteosclerosis (ivory vertebra) has been described (9). Osteosclerosis is presumed to be owing to reactive new bone formation and osteoid deposition on dead bone (6). Expansion of the involved bone is unusual (10). The disk spaces are usually preserved, but in rare cases can become widened (11). Extension into the spinal canal is frequent, as are paraspinal soft-tissue

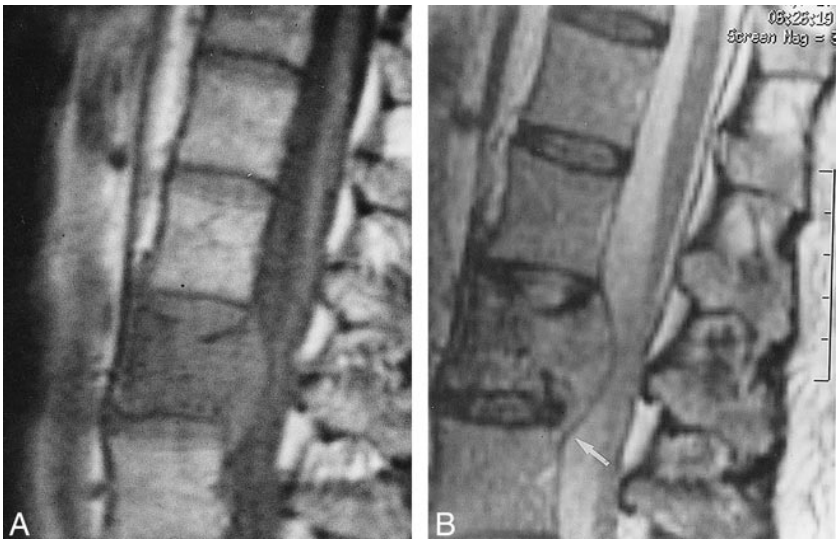

FIG 9. *A,* Proton density–weighted sagittal image of 53-year-old woman with aggressive VH of L3 vertebra. There is decrease of signal in L3 vertebral body. There is a large, homogeneous, low-signal extraosseous mass within spinal canal compressing thecal sac. There is growth of tumor superiorly and inferiorly along posterior aspect of L3 vertebral body. Note that there is preservation of intervertebral disk spaces.

B, T2-weighted sagittal images (from same patient as 9A) shows that signal in extraosseous component increases on T2-weighted image. T2-weighted image better shows how tumor extends beyond inferior disk space (*arrow*).

masses. Calcification of the soft-tissue mass is uncommon (10).

Findings on MR images are also nonspecific. Ewing's sarcoma has been described as having decreased (1) to intermediate (12) signal on T1-weighted images and increased signal intensity on T2-weighted images (1, 12). The intramedullary portion of the tumor may be homogeneous or heterogeneous, depending on the histologic presentation. Tumors with large amounts of blastic or reactive bone appear heterogeneous, whereas those consisting of neoplastic cells and no reactive bone appear homogeneous (12). The extraosseous component is often homogeneous because it is often devoid of calcification and new bone formation (12).

Early diagnosis and treatment are important, as a 100% local control rate and 80% disease-free survival in proximal spinal primaries has been reported (8). For progressive neurologic symptoms from epidural compression or if there is evidence of spinal instability, prompt surgical decompression is essential to prevent irreversible neurologic defects (7). In patients who are without severe or progressive neurologic deficits, chemotherapy preloading can be attempted first, with surgery or radiation therapy or both tailored to the individual patient (7).

The variable radiographic appearance of primary ES of the spine has been previously mistaken for many other disorders (1). The presence of back pain with radiation to the lower extremities or objective neurologic deficit has led some to misdiagnose ES as lumbar disk disease or tuberculosis (9). Osteolysis with complete vertebral collapse and intact disk spaces simulates vertebra plana, suggesting the diagnosis of eosinophilic granuloma (1, 2). Expansion of a transverse process and calcification in a paraspinal mass (both rare manifestations of ES) have led to misdiagnoses of aneurysmal bone cyst and neurogenic tumor, respectively (10). Other ES tumors have been misdiagnosed as giant cell tumor, metastasis, lymphoma, and osteogenic sarcoma (1).

Although primary ES of the spine is rare, vertebral hemangiomas (VHs) are the most common benign tumors of the spinal column, and have been found in up to 11% of spines in autopsy studies (13). Although round cell tumor was included in our differential at the time, we believed that uncommon mainfestations of common disorders (VH) were more likely than uncommon presentations of uncommon disorders (ES).

Most VHs are asymptomatic, although some exhibit a more aggressive clinical course that can result in vertebral body compression fracture and compression of neural structures due to epidural mass effect from the tumor or hemorrhage (14). Asymptomatic VHs show fatty intervening stroma with little or no hypervascularity on angiograms. In comparison, compressive VHs show no stromal fat with increased soft-tissue attenuation on CT scans and hypervascularization on angiograms (15). It is thought that the aggressiveness of a VH is caused by the increased vascular stroma (15).

On CT scans, the thickened spinal trabeculae associated with VH are seen as punctate areas of sclerosis between areas of fat or vascular stroma, resulting in a polka-dot appearance to the vertebrae on cross-sectional imaging (13, 14). VHs classically appear on MR images as high-signal lesions on T1- and T2-weighted images, although ''aggressive'' vertebral hemangiomas manifest as low-signal lesions on T1-weighted images because of decreased fat content and an increased vascular stroma (16).

In a review of 57 solitary VHs, Laredo et al looked at plain-film and CT criteria to identify asymptomatic VHs from those that compressed the cord (ie, aggressive). They found the following six features that were more common with aggressive VHs: 1) involvement of the entire vertebral body; 2) extension into the neural arch; 3) cortical ex-

pansion; 4) thoracic location (T3–T9); 5) irregular honeycomb pattern; and 6) a soft-tissue mass. They concluded that the two different types of VH can be differentiated by a scoring system in which three or more of the above criteria occurring in association with nerve root pain should raise the suspicion of an active VH. This would require the use of selective arteriography, followed by embolization of the feeding arteries, if indicated (17). As our case had many of these features on cross-sectional imaging and there was no evidence of metastatic disease, we were erroneously led to consider an aggressive VH as our top diagnosis.

In retrospect, the degree of epidural extension may have helped us distinguish this ES from an aggressive VH. Primary spinal ES usually extends beyond the affected vertebral body into the posterior spinal elements, paraspinal soft tissues, and extradural space; however, this may be seen with aggressive VHs (Fig 9). The paraspinal component is often larger than the intraosseous lesion. Mohan and colleagues argue that extension of the paraspinal component above and below the involved vertebra also helps differentiate ES from other lesions (9).

In conclusion, primary ES of the spine may have a variety of appearances on imaging studies, including a coarse trabecular pattern of osteosclerotic and osteolytic destruction that is characteristic of VH, as demonstrated in this case. Therefore, it should be considered in the differential diagnosis in any pediatric patient with a solitary destructive lesion of vertebrae.

Acknowledgments

The authors would like to thank Drew Olsen, M.D. for his assistance with the histologic analysis of this case.

References

1. Amour TE, Hodges SC, Laakman RW, Tamas DE. **Other primary extradural tumors.** In: *MRI of the Spine*. Amour TE, Hodges SC, Laakman RW, Tamas DE, eds, New York: Raven Press; 1994: 509–516
2. Grubb MR, Currier BL, Prichard DJ, Ebersold MJ. **Primary Ewing's sarcoma of the spine.** *Spine* 1994;19:309–311
3. Whitehouse GH, Griffiths GJ. **Roentgenological aspects of spinal involvement by primary and metastatic Ewing's tumor.** *J Can Assoc Radiol* 1976;27:290–297
4. Twohig M, Sze G. **Spinal tumors.** In: *Magnetic Resonance Imaging of Children.* Cohen MD, Edwards, MK, eds. Philadelphia: BC Decker Inc; 1990:463–498
5. Fechner RE, Mills SM. **Small cell sarcomas.** In: *Tumors of the Bones and Joints.* Fechner RE, Mills SM, eds. Washington, DC: Armed Forces Institute of Pathology; 1993:87–202
6. Resnick D, Kyriakos M, Greenway GD. In: *Diagnosis of Bone and Joint Disorders.* Resnick D, ed. Philadelphia: W.B. Saunders; 1994:3628–3938
7. Sharafuddin MJ, Haddad FS, Hitchon PW, Hadddad SF, EL-Khoury GY. **Treatment options in primary Ewing's sarcoma of the spine: Report of seven cases and review of the literature.** *Neurosurgery* 1992;30:610–619
8. Pilepich VM, Vietti TJ, Nesbit ME, et al. **Ewing's sarcoma of the vertebral column.** *Int J Radiation Oncology Biol Phys*, 1981; 7:27–31
9. Mohan V, Sabri T, Gupta RP, Das DK. **Solitary ivory vertebra due to primary Ewing's sarcoma.** *Pediatr Radiol* 1992;22: 388–390
10. Wienstien JB, Siegel MJ, Griffith RC. **Spinal Ewing sarcoma: misleading appearences.** *Skel Radiol* 1984;11:262–265
11. Lampaert A, Velde VD, **Crommelinck. Primary Ewing's Sarcoma of the spine: a rare location? Report of four cases.** *JBR-BTR* 71:463–489
12. Moore SG, Dawson KL. **Tumors of the musculoskeletal system.** In: *Magnetic Resonance Imaging of Children.* Cohen MD, Edwards, MK eds. Philadelphia: BC Decker Inc. 1990:825–912
13. Murphey MD, Fairbairn JK, Parman LM, Baxter KG, Parsa MB, Smith SW. **From the Archives of the AFIP: Musculoskeletal angiomatous lesions radiologic-pathologic correlation.** *RadioGraphics* 1995;15:893–917
14. Colombo N, Berry I, Norman D. **Vertebral tumors.** In: *Imaging of the Spine and the Spinal Cord.* Manelfe C, ed. New York: Raven Press; 1994:445–488
15. Laredo JD, Assouline E, Gelbert F, Wybier M, Merland JJ, Tubiana JM. **Vertebral hemangiomas: Fat content as a sign of aggressiveness.** *Radiology* 1990;177:467–472
16. Amour TE, Hodges SC, Laakman RW, Tamas DE. **Hemangiomas.** In: *MRI of the Spine.* Amour TE, Hodges SC, Laakman RW, Tamas DE, eds. New York: Raven Press; 1994:467–474
17. Laredo JD, Reizine D, Bard M, Merland JJ. **Vertebral hemangiomas: Radiologic evaluation.** *Radiology* 1986;161:183–189